FERMILAB-CONF-08-125-E

CURRENT NUMI/MINOS OSCILLATION RESULTS

A. HABIG,
for the MINOS Collaboration
Department of Physics, University of Minnesota Duluth
10 University Dr., Duluth, MN 55812 USA

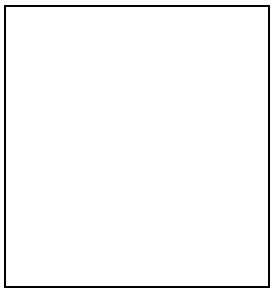

The MINOS experiment is now making precise measurements of the ν_μ disappearance oscillations seen in atmospheric neutrinos, and will extend our reach towards the so far unseen θ_{13} by looking for ν_e appearance in the ν_μ beam. It does so by using the intense, well-understood NuMI neutrino beam created at Fermilab and observing it 735km away at the Soudan Mine in Northeast Minnesota. Results from MINOS' first two years of operations will be presented.

1 Introduction

Results from the Super-Kamiokande experiment used neutrinos produced by cosmic ray interactions with the upper atmosphere to show that muon neutrinos (ν_μ) of energies from a few hundred MeV through TeV oscillate to tau neutrinos (ν_τ) as they travel the tens to thousands of kilometers through the earth to the detector [1]. This implies that neutrinos have mass, a finding of fundamental importance to both particle physics and astrophysics. The K2K experiment used a beam of neutrinos shot across Japan to the Super-K detector to confirm this result in a controlled fashion [2]. The MINOS (Main Injector Neutrino Oscillation Search) experiment has unambiguously confirmed this result. MINOS will precisely measure the oscillation parameters using the intense, well-calibrated NuMI (Neutrinos at the Main Injector) beam of neutrinos generated at Fermilab. This neutrino beam was commissioned in early 2005 and is aimed toward the Soudan Underground Physics Laboratory in northeastern Minnesota. The neutrinos are observed by similar magnetized steel/scintillator calorimeters near their origin in Fermilab and after traveling 735 km to Soudan.

Differences in signals between the two detectors have already provided the best measurement yet of $\nu_\mu \leftrightarrow \nu_\tau$ flavor oscillations in a long-baseline accelerator experiment, using the first two years operation of the NuMI neutrino beam [3]. With more data, MINOS will reach its projected

sensitivity to this mixing, improved sensitivity to any sub-dominant ν_e modes (a probe of θ_{13}) and high statistics neutrino cross section studies. This paper presents the current result on $\nu_\mu \leftrightarrow \nu_\tau$ oscillations, the first look at the spectrum of neutral current ("NC") events in the MINOS near detector, the methods which will be used to search for ν_e appearance, and new data-driven sensitivities to θ_{13}.

1.1 The NuMI Beam

The NuMI neutrino beam [4] uses 120 GeV protons from the Main Injector synchrotron at Fermilab incident upon a graphite target. 90% of the primary protons interact over the two interaction-length long target, producing showers of π and K mesons. These showers are focused by a pair of parabolic aluminum "horns", pulsed electromagnets carrying current sheaths which focus the mesons into a beam. This beam is sent down a 1 m radius, 675 m long decay pipe. While in this pipe the mesons have a chance to decay into muons and muon neutrinos, but few of the muons have enough time to further decay before they are absorbed at the end of the pipe, a decay which would produce electron and anti-muon neutrinos. The resulting neutrino beam is thus composed of approximately 92.9% ν_μ, 5.8% $\overline{\nu}_\mu$, 1.2% ν_e and 0.1% $\overline{\nu}_e$ for the low-energy ("LE") beam configuration.

The target and horns are movable with respect to each other, allowing different focusing optics. The result is a beam which is configurable in energy, as seen in Fig. 1. The LE configuration ("a") produces a spectral peak closest to the first oscillation minima, given the oscillation parameters measured by Super-K and the 735 km baseline to the far detector. Moving the target with respect to the horns produces the "pME" ("b") and "pHE" ("c") beams peaked at medium and higher energies. While not at ideal energies for the ν_μ disappearance analysis, these beams are much more intense ($\sim$970 and 1340 neutrino events at the far detector per 10^{20} protons on target, compared to $\sim$390 for the LE beam) and provide extra handles when using the near detector data to model the beam's properties. The MINOS near detector is only a km away from the target, so even the LE beam produces around 10^7 neutrino interactions per 10^{20} protons on target, a very high statistics sample of this weakly interacting particle. The beam currently delivers 3.1×10^{12} protons over a 12 μs spill every 2.2 s for an average power of 270 kW. The NuMI beam has been operational since march of 2005, and to date (of this conference, March 2008) has delivered more than 4×10^{20} protons on target.

1.2 The MINOS Detectors

The MINOS experiment observes the NuMI beam with two detectors, "near" and "far". A third "calibration" detector was exposed to beams of protons, pions, electrons and muons from the the CERN PS [6] to determine detector response. The near detector at Fermilab is used to characterize the neutrino beam with high statistics and is 1 km downstream from the NuMI target. The far detector is an additional 734 km downstream. This experiment compares the spectra of different types of neutrino interactions at these two detectors to test oscillation hypotheses.

All three MINOS detectors are steel-scintillator sampling calorimeters [5] made of alternate planes of 4.1×1 cm cross section plastic scintillator strips and 2.54 cm thick steel plates. The near and far detectors have magnetized steel planes. The calibration detector was not magnetized as the incoming particle momenta were known. The extruded polystyrene scintillator strips are read out with wavelength-shifting fibers and multi-anode photomultiplier tubes. The far detector is 705 m underground in Soudan, MN, in a disused iron mine currently operated as a State Park by the Minnesota Department of Natural Resources. The 5,400 metric ton far detector consists of 486 8 m-wide octagonal steel planes interleaved with planes of plastic scintillator strips.

The 282 plane, 980 metric ton MINOS near detector is located at the end of the NuMI beam facility at Fermilab in a 100 m deep underground cavern. While the NuMI beam has diverged to

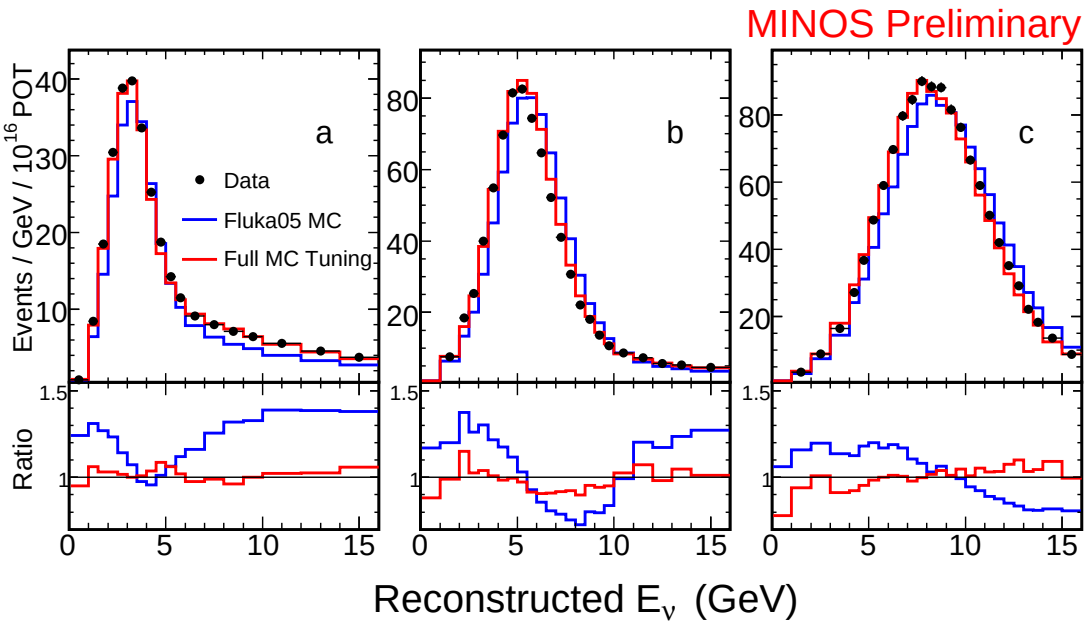

Figure 1: The measured energy spectrum of neutrinos from the NuMI beam observed by the MINOS near detector (top) and the ratios of data and expectations (bottom). Data points are the black dots, the untuned MC predictions are the blue curves, and MC predictions after tuning on hadronic x_F and p_t simultaneously across many different beam configurations are the red curves. The three plots are for three of the different NuMI beam configurations, a) LE; b) pME; and c) pHE.

a mile wide at Soudan, at the near detector it is mostly contained in a meter-wide area, allowing a smaller detector and a factor of 10^6 higher neutrino rate.

The much smaller calibration detector was used to measure the detailed responses of the MINOS detectors in a charged-particle test beam. This 12 ton detector consisted of 60 planes of unmagnetized steel and scintillator, each 1×1 m^2 [6]. It measured the energy and topological responses expected in the the near and far detectors, including the different electronics used in both larger devices. The energy responses of the three MINOS detectors were normalized to each other by calibrating with cosmic-ray muons.

2 Data Analysis

MINOS beam-based data is analyzed using a "blind analysis". This method avoids looking at the actual data containing the physics being studied until the very end, removing potential biases and increasing confidence in the final result. Monte Carlo ("MC") predictions are tuned and verified using data not sensitive to the physics in question (*e.g.* near detector data which is at too short a baseline to have experienced oscillations), and analysis cuts and techniques developed solely using simulated data. Only after these techniques are optimized and set are the sensitive data (in this example, the far detector oscillated data) revealed. All three of the results discussed in this paper are blind analyses, and are at different stages in the process.

The first step, common to all beam-based analyses, is to understand the beam itself. A detailed MC tracks simulated particles through the proton-meson-neutrino chain described in Sec. 1.1, to create an expected neutrino spectrum at the near detector. This MC is developed and crosschecked with information from the NuMI beam monitoring system, including a hadron monitor in the absorber at the end of the decay pipe and three muon monitors further downstream. As can be seen in the blue curves in Fig. 1, this does a decent but not perfect job of predicting the observed neutrino spectra in the near detector. Further tuning is done

by reweighting hadronic x_F and p_t in the MC simultaneously across seven different beam configurations and comparing to real near detector data, as the hadronic models have the most theoretical uncertainty. Four additional beam configurations (with different horn focusing currents) beyond those shown are included in this fit, and the resulting tuned predictions are the red line in Fig. 1. With the MC truth information in hand, a far detector prediction can be made by applying changes due to mundane things like geometrical and kinematic factors, or more exciting things like neutrino oscillations.

With a beam MC prediction in hand, topological features in the near detector data can be examined. Fitters to find tracks and neutrino interaction vertices, shower-finding algorithms, and particle identification ("PID") routines can be developed, tested, and calibrated using near detector data, the beam MC, and cosmic ray data at both detectors. Once an analysis can correctly matches the real data and the MC data, efficiencies and purities of the resulting sample can be extracted from the MC truth information, systematic uncertainties estimated, and expected sensitivity curves to the final physics parameters calculated. Only at this point is the "box opened", the far detector data run through the analysis, and the hypotheses tested to see what Mother Nature is really doing..

2.1 Atmospheric sector neutrino oscillations

The main goal of the MINOS experiment is a precision measurement of the ν_μ disappearance oscillations first observed in atmospheric neutrinos. In the Standard Model, neutrinos are assumed to be massless and direct neutrino mass measurements have been able to establish only upper limits to their masses. Quantum mechanics predicts that if neutrinos do indeed possess a non-zero mass, then although the neutrinos are created and interact via the weak force as flavor eigenstates (corresponding to the flavors of leptons: electrons, muons and tauons – ν_e, ν_μ, ν_τ) they propagate through space as mass eigenstates (ν_1, ν_2, ν_3). The flavor eigenstates are simple superpositions of the mass eigenstates [7]. If the neutrinos have differing masses, then the flavor of the neutrino varies as these states drift into and out of phase with each other while propagating through space, thus "oscillating" in flavor. For the case of two-flavor oscillations (*e.g.* $\nu_\mu \leftrightarrow \nu_\tau$) the probability that a neutrino produced via the weak interaction in the muon flavor state has oscillated to, or will be detected as, the tau state by the time it interacts is:

$$P_{\nu_\mu \to \nu_\tau} = \sin^2 2\theta_{23} \sin^2 \left(\frac{\Delta m^2_{32} L}{4E_\nu} \right), \tag{1}$$

where the properties of nature being probed are the amplitude or mixing angle θ_{23} and $\Delta m^2_{32} = m^2_3 - m^2_2$. The observable quantities are the energy of the neutrino E_ν and the distance the neutrino has traveled, also called the "baseline" L. Observation of neutrino flavor oscillations which vary as L/E implies that both the terms Δm^2_{32} and $\sin^2 2\theta_{23}$ are non-zero, and that at least one of the participating neutrino flavors has mass.

The analysis techniques discussed above were applied to data from the start of the NuMI beam through March 2007, totaling 2.947×10^{20} "LE" beam protons on target ("pot"). This includes the previously published [3] 1.27×10^{20} pot, although the analysis has been improved for both old and new data. A 3% larger fiducial volume was used, the data reconstruction was improved and retained 4% more good neutrinos, and the PID algorithm was revamped to provide both better purity and efficiency. The resulting sample of 563 ν_μ charged current ("CC") neutrino interactions is plotted as a function of reconstructed neutrino energy on the left of Fig. 2, and a ratio with expectations (right) shows an energy dependent deficit.

Equation 1 was applied on a two-dimensional $(\Delta m^2, \sin^2 2\theta)$ grid to the MC predictions, and a χ^2 formed compared to the data. Estimated systematic errors are less than the current statistical errors and applied as penalty terms to the χ^2. The best fit value for the oscillation

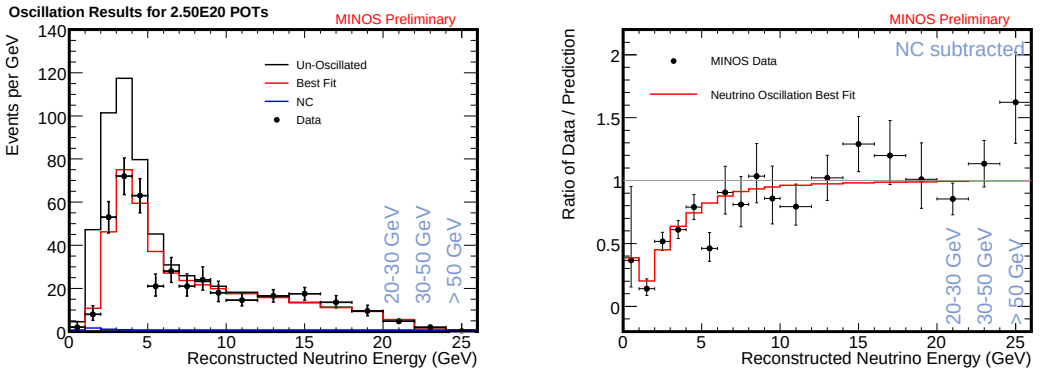

Figure 2: (Left) The observed ν_μ energy spectrum seen in the MINOS beam at the far detector for an exposure of 2.947×10^{20} pot. Black crosses are the data with statistical error bars, the black line the null hypothesis, the red line the expectations of the best fit oscillation scenario of $\left|\Delta m^2_{32}\right| = 2.38^{+0.20}_{-0.16} \times 10^{-3}\,\mathrm{eV}^2$, $\sin^2 2\theta_{23} = 1.00_{-0.08}$, and the blue line (barely visible in the first few energy bins) the expected NC contamination. (Right) The same quantities expressed as a ratio of observed over expected null hypothesis.

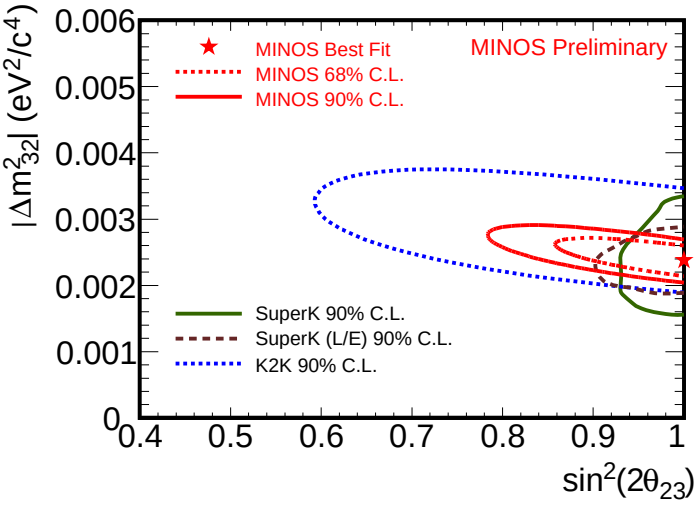

Figure 3: The allowed regions in the oscillation parameter space of Eq. 1, obtained by fitting reweighted MC predictions to the MINOS data in Fig. 2. MINOS results (red) at 68% and 90% c.l. are compared to Super-K results (green) [1, 8] and K2K results (blue) [2] at 90% c.l.

parameters to the MINOS data are $\left|\Delta m^2_{32}\right| = 2.38^{+0.20}_{-0.16} \times 10^{-3}\,\mathrm{eV}^2$ and $\sin^2 2\theta_{23} = 1.00_{-0.08}$, and the resulting 68% and 90% confidence limit contours are shown in Fig. 3.

2.2 Neutral Current Interactions

The ν_μ disappearance results discussed in the previous section (2.1) use topological information to form a PID to select a sample of CC ν_μ neutrinos, on the assumption that the flavor they are disappearing to is ν_τ, an active flavor of neutrino, unobserved in MINOS since the bulk of the NuMI neutrino flux is at energies below τ production threshold. However, if the second flavor of neutrino is a non-standard model sterile neutrino (one which experiences no weak interactions), the disappearance signature could look the same with very different underlying physics.

NC neutrino interactions hold the key to separating these two scenarios in MINOS. Active neutrinos of any flavor can experience a NC Z^0 exchange with a nucleon in the detector and produce a diffuse electromagnetic shower from the resulting π^0 decay to $\gamma\gamma$. A hypothetical sterile neutrino would not, so if some fraction of the ν_μ signal is changing to ν_s, the NC spectrum

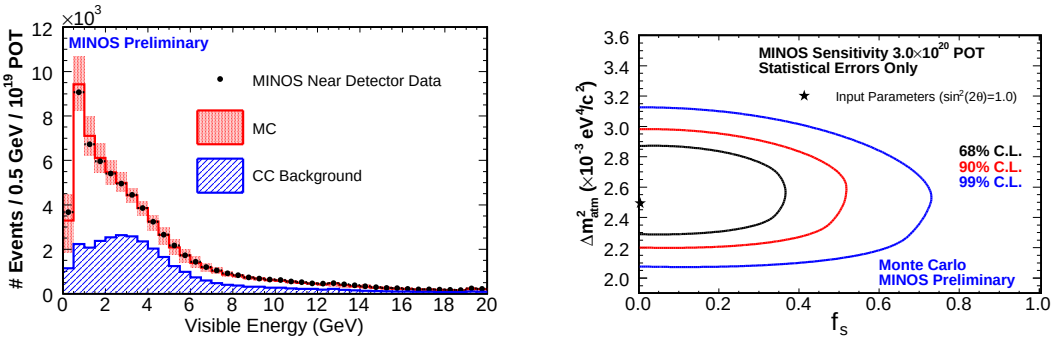

Figure 4: (Left) The spectrum of NC-selected events seen in the near detector for an exposure of 3.0×10^{20} pot. The black dots are the reconstructed neutrino data, the red boxes the expected signal (systematic error bands as the area), and the blue region the expected CC contamination to this NC signal. (Right) The projected sensitivity to a fraction of $\nu_m u$ disappearance to sterile rather than active neutrinos, as a function of Δm^2.

would be distorted and NC flux reduced. A simple set of cuts has been applied to the near detector data to select a NC-rich sample of neutrino interactions for further study. Short tracks (<60 planes) are selected, then events with either no track at all or no track beyond five planes from the shower are chosen. The resulting spectrum of NC near detector neutrino interactions is shown in the left of Fig. 4, with projected limits on f_s (the fraction of disappearance to ν_s shown on the right if no NC disappearance is observed.

This analysis is in the middle of the "blind" analysis scheme discussed above. Having chosen a set of topological cuts to select a NC signal, data and MC comparisons are being made with near detector data to verify that they are well understood before looking at the far detector data to see what the potentially oscillated signal might look like. This analysis is expected to be complete the summer of 2008.

2.3 Sensitivity to ν_e appearance

A third possibility for which particle the ν_μ's are disappearing to is ν_e. We know that there could be some natural mixing between all three active flavors of neutrinos, and the amplitude of this is parametrized as θ_{13}. The Chooz reactor experiment saw no evidence of the converse ν_e disappearance at short baselines to establish an upper limit on θ_{13} [9]. However, the presence of ν_e in the MINOS far detector beyond the low (1.3%) level inherent to the NuMI beam could provide evidence for a non-zero θ_{13} below the Chooz limit, if the background of hadronic showers masquerading as electromagnetic showers can be overcome. The PID algorithm used for ν_e selection uses a neural net technique to pick out ν_e-induced showers. At the near detector the baseline is far too short for ν_μ to have oscillated to ν_e, so any observed ν_e must either be inherent in the beam or the mis-reconstructed hadronic showers in question. To improve the MC estimations of what the levels of these backgrounds might really be in the MINOS detectors, data-driven sensitivity studies have been performed by close examination of near detector data tagged as ν_e events.

Two methods are used in these studies. The first is to take the well-understood class of CC events and subtract out those parts of the event associated with the muon track, leaving only any hadronic component near the interaction vertex caused by the nucleon's share of the interaction energy. These "Muon-Removed Charged Current" (MRCC) events which are mis-classified as ν_e interactions are exactly the sort of electromagnetic-dominated hadronic showers that form a large part of the background for a ν_e appearance search. There is a 20% discrepancy between the data and the MC predictions in both the standard ν_e and MRCC samples with the MC overestimating the background. Comparisons of standard data and MC shower topological

distributions disagree in the same way as does MRCC data with MRCC MC, confirming that hadronic shower modeling is a major component of the disagreement. The MRCC sample is thus used to make and ad-hoc correction to the model to NC events per bin, taking the beam ν_e from the well-understood beam MC.

A second method for estimating the ν_e background from hadronic showers uses comparisons between the neutrino beam produced when the focusing horn's current is turned off and the standard LE beam. The actual composition of the selected ν_e events is quite different in the two cases, allowing for the algebraic deconvolution of the different background components by expressing the total number as a sum of the different parts in the case of each beam:

$$\begin{aligned} N_{on} &= N_{NC} + N_{CC} + N_e \\ N_{off} &= r_{NC}N_{NC} + r_{CC}N_{CC} + r_eN_e \end{aligned} \tag{2}$$

where N_{NC} and N_{CC} are the numbers of background events present originating from CC or NC interactions, N_e the inherent beam ν_e taken from the beam MC, and the r's the ratios that hold the differences between the two equations, $r_{NC(CC,e)} = N^{off}_{NC(CC,e)}/N^{on}_{NC(CC,e)}$. The horn on/off ratios are extracted bin-by-bin in energy from the MC, are independent of hadronic modeling, and match well between data and MC. These fractions can then be applied to the data itself to extract the components of the background, indicating that there is 24% too much CC and 28% too much NC backgrounds in the MC. Checks with a third (pHE) beam produce similar results, and both are compatible with the corrections from the MRCC method outlined above.

These data-drive backgrounds can then be extrapolated to the far detector for use in establishing the sensitivity expected when using a ν_e appearance search to try and measure θ_{13}. These sensitivities are presented in Fig. 5 for three different exposures, the current 3.25×10^{20} pot as well as those expected for next two years. The systematic errors for the current background estimation are found to be 10%, and with more data and study it is projected to fall to 5% for future years. The unknown variable of CP-violating δ contributes to ν_e appearance through the matter effects on the beam between Fermilab and Soudan, so the y-axis of these plots shows the effect of this δ. The actual sign of $\Delta m^2 32$ also enters in, making this analysis less sensitive for the "inverted" mass hierarchy. However, after two more years of exposure MINOS will be sensitive to θ_{13} below the Chooz limit for most combinations of δ and mass hierarchy. The next step in this blind analysis is to examine far detector data in "sidebands" that allow verification of techniques without being sensitive to actual ν_e appearance.

3 Summary

The MINOS long-baseline neutrino experiment has been receiving 735 km baseline neutrinos from the NuMI neutrino beam since early 2005. The primary experimental goal of a precision measurement of the $\nu_\mu \leftrightarrow \nu_\tau$ disappearance oscillation parameters has been achieved. With the first 2.5×10^{20} protons on target, $|\Delta m^2_{32}| = 2.38^{+0.20}_{-0.16} \times 10^{-3}\,\mathrm{eV}^2$ and $\sin^2 2\theta_{23} = 1.00_{-0.08}$. This is about a quarter of the expected final exposure, which will allow fine distinction between alternative disappearance hypotheses such as decoherence and neutrino decay to be made in the future. The first measurement of the spectrum of neutral current neutrino interactions has been made in the high-statistics near detector data. When the blind analysis of the corresponding far detector is complete later this year, it will be sensitive to a sterile neutrino fraction $f_s \leq 0.5$ at 90% c.l. Again using the near detector data, a data-driven background estimate to the ν_e appearance analysis has been made. This yields a sensitivity estimates comparable to the Chooz limit for the currently available exposure of 3.25×10^20 protons on target, reaching several times lower than this limit as soon as next year.

The NuMI beam and the MINOS experiment are going strong, the data and beam are well understood, and quality results are being produced. The next year should see the completion

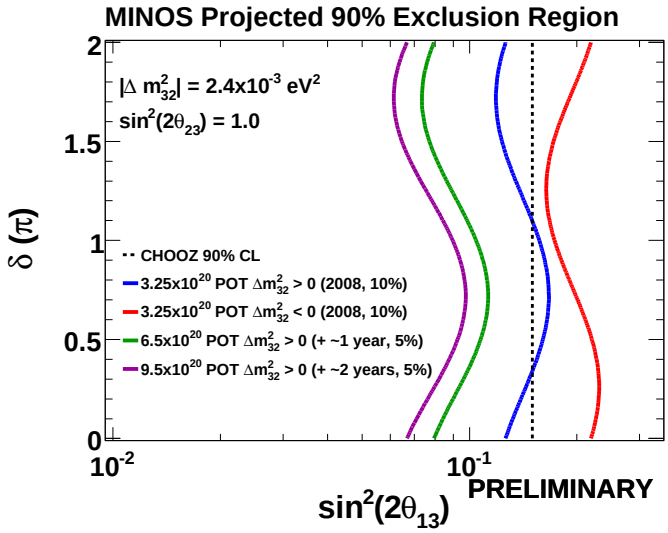

Figure 5: Projected 90% c.l. limits on θ_{13} as a function of CP-violating δ from the MINOS experiment in the absence of a ν_e appearance signal. These limits use data-driven background estimates from the near detector. The vertical dashed line is the Chooz limit [9]. The rightmost (red) curve is the limit using the current exposure in the case of an inverted mass hierarchy, the neighboring (blue) curve is the limit from the same exposure if nature has a normal neutrino mass hierarchy. The two curves on the left are the progressively more sensitive normal hierarchy limits for the increased NuMI beam exposure over the next two years. The corresponding inverted hierarchy curves for these two scenarios are not shown for ease of viewing, but improve over the current exposure limits in a corresponding manner to the normal curves.

of initial analyses on all major experimental goals and the continued refinement of the precision parameter measurement of neutrino oscillations in the atmospheric neutrino sector.

Acknowledgments

We thank the Fermilab staff and the technical staffs of the participating institutions for their vital contributions. This work was supported by the U.S. Department of Energy, the U.S. National Science Foundation, the U.K. Science and Technologies Facilities Council, and the State and University of Minnesota. We gratefully acknowledge the Minnesota Department of Natural Resources for their assistance and for allowing us access to the facilities of the Soudan Underground Mine State Park and the crew of the Soudan Underground Physics laboratory for their tireless work in building and operating the MINOS detector.

References

1. Y. Ashie *et al.*, Phys. Rev. D **71**, 112005 (2005).
2. M. H. Ahn *et al.*, Phys. Rev. D **74**, 072003 (2006).
3. P. Adamson *et al*, Phys. Rev. D **77**, 072002 (2008).
4. A. G. Abramov *et al.*, Nucl. Instrum. Meth. **A385**, 209 (2002).
5. D. G. Michael *et al* submitted to Nucl. Instrum. Meth. **A** (2008).
6. P. Adamson *et al*, Nucl. Instrum. Meth. **A566**, 119 (2006).
7. B. Pontecorvo, Sov. Phys. JETP **6**, 429 (1957); Zh. Eksp. Teor. Fiz. **33**, 549 (1957).
8. Y. Ashie *et al.*,Phys. Rev. Lett **93**, 101801 (2004).
9. M. Apollonio *et al.*, Phys. Lett. **B466**, 415 (1999).